MECHANICS 2025. Vol. 35. Issue 4. Pp. 601–618.

MSC2020: 34A34, 76Bxx, 37J12

© *E. M. Artemova, D. A. Lagunov*

THE MOTION OF A BALANCED CIRCULAR FOIL IN THE FIELD OF FIXED POINT SOURCES

This paper is concerned with the motion of a circular foil in an ideal incompressible fluid containing two fixed point sources. It is shown that the study of such a system reduces to investigating the motion of a material point (the geometric center of the foil) in a potential field. Fixed points of the system corresponding to stationary configurations of the foil in absolute space are found. An analysis is made of the limiting case with sources whose intensities are opposite in sign, but have the same absolute value and which are contracted to a single point, that is, the motion of the foil in the field of a fixed dipole is considered. It is shown that in this case the system is integrable, and a complete analysis of the system is carried out.

Keywords: ideal fluid, circular foil, point source, Hamiltonian form.

DOI: 10.35634/vm250406

Introduction

The study of the motion of rigid bodies in a fluid is one of the fundamental problems in theoretical and applied hydrodynamics. The case of plane-parallel motion of a rigid body is of particular significance in this field. This approach makes the investigation of the dynamics and control much simpler. For example, the authors of [1, 2] perform a numerical simulation of the motion of a rigid body in a viscous fluid. The results of two-dimensional simulation of a flapping wing in [1] agree with the three-dimensional experiment and the two-dimensional simulation performed in [3].

In addition to a viscous fluid, one often considers the model of an ideal incompressible fluid because it allows simplifying the solution of the hydrodynamical problem and reducing the investigation to analysis of the equations of classical mechanics. For example, Ref. [4] considers the motion of articulated bodies, which propel themselves by changing their shape. The authors of [5–7] develop models featuring the motion of a body in a fluid using various internal mechanisms (a rotor or moving masses). Such models make it possible to reproduce the characteristic features of the dynamics of a mobile robot moving on the water surface. However, for a quantitative agreement with experiment the model requires additional correction.

In addition to body motion in a fluid under the action of some internal mechanisms, attention is also given to the influence of the singularities of the flow (for example, vortices) on rigid body motion. For example, Ref. [8] analyzes the motion of a circular foil with two vortices and shows that, under some conditions on the system's parameters, the problem is integrable. In [9, 10], equations of motion of a circular foil with an arbitrary number of vortices are derived. The influence of an attached vortex on the motion of an elliptic foil was discussed in [11]. Sources/sinks or vortex sources may also be considered as singularities of the flow. Refs. [12–14] are devoted to the motion of a circular and an elliptic foil in the field of one fixed point source.

This paper is a continuation of [12–14] and examines the motion of a balanced circular foil in the field of two fixed point sources. Section 1 presents the construction of a mathematical model. Section 2 analyzes particular solutions to equations describing the motion of the foil and addresses the question of integrability of these equations. Subsections 2.1 and 2.2 are concerned with particular cases: sources of the same intensity and sources whose intensities have the same

absolute value, but are opposite in sign. Section 3 examines the limiting case where sources whose intensities are opposite in sign contract to a single point, i. e., it examines the system of a circular foil in the field of a fixed dipole.

§ 1. Mathematical model

Consider the plane-parallel motion of a circular foil of radius R in an ideal incompressible fluid. For this system we make the following assumptions:

1° The circular foil is balanced, i. e., the center of mass is at the geometric center.

2° The fluid contains two fixed point sources with constant intensities q_1 and q_2, respectively. The motion of the fluid is potential everywhere except at points at which the sources are located.

3° The motion of the fluid about the foil is irrotational. At infinity its velocity is zero.

To describe the motion of a circular foil, we introduce a fixed coordinate system Oxy attached to the complex plane z as shown in Fig. 1. Let (x_c, y_c) denote the geometric center of the foil. Without loss of generality, we choose the position of the singularities at points $(\pm a, 0)$, where $a > 0$. This can always be achieved by choosing a coordinate system.

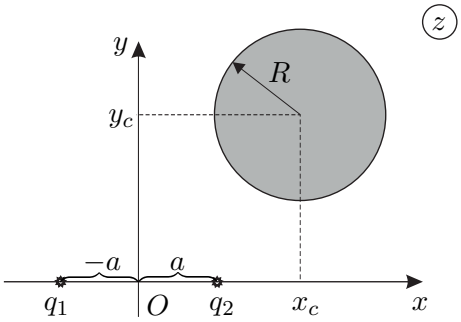

Fig. 1. Schematic representation of the system

Under the assumptions made above, the motion of the fluid can be described using a complex potential of the following form:

$$w = -\frac{uR^2}{z - z_c} + \frac{q_1}{2\pi}\ln(z + a) + \frac{q_2}{2\pi}\ln(z - a) + \\ + \frac{q_1}{2\pi}\ln\left(\frac{R^2}{z - z_c} + \overline{a + z_c}\right) + \frac{q_2}{2\pi}\ln\left(\frac{R^2}{z - z_c} - \overline{a - z_c}\right),$$

where $z_c = x_c + iy_c$ is the coordinate of the center of the circular foil, $u = \dot{z}_c = \dot{x}_c + i\dot{y}_c$ is the velocity of the center of the circular foil, and the bar denotes complex conjugation.

The torque (relative to the center of mass of the foil) acting on the circular foil is zero. Thus, to derive equations of motion for the circular foil, it is necessary to define only the force due to the pressure from the fluid on the foil. The force can be calculated by the formula proposed by Sedov [15]:

$$F_x + iF_y = \overline{\frac{i\rho}{2}\oint\limits_C \left(\frac{dw}{dz}\right)^2 dz} + \frac{d}{dt}\left(\rho S u + i\rho \oint\limits_C z\frac{dw}{dz}\,dz\right), \tag{1.1}$$

where F_x, F_y are the projections of the force onto the axes of the coordinate system Oxy, $S = \pi R^2$ is the area of the foil, C is the contour of the foil, and ρ is the fluid density. Using the formula (1.1), an explicit expression for the force was obtained:

$$F_x + iF_y = -\rho\pi R^2 \dot{u} + \frac{\rho q_2^2 R^2 (a - z_c)}{2\pi |a - z_c|^2 \big(|a - z_c|^2 - R^2\big)} - \frac{\rho q_1^2 R^2 (a + z_c)}{2\pi |a + z_c|^2 \big(|a + z_c|^2 - R^2\big)} + \\ + \frac{\rho q_1 q_2 R^2 (a + z_c)}{2\pi |a + z_c|^2 \big((a - z_c)(\overline{a + z_c}) + R^2\big)} - \frac{\rho q_1 q_2 R^2 (a - z_c)}{2\pi |a - z_c|^2 \big((a + z_c)(\overline{a - z_c}) + R^2\big)}.$$

The equations of motion of the circular foil can be represented as the classical Newton equations

$$m\ddot{x}_c = F_x, \qquad m\ddot{y}_c = F_y. \tag{1.2}$$

This system of equations is closed and completely describes the motion of the circular foil in the presence of two fixed sources.

Lagrangian form. The equations of motion of the foil (1.2) can be represented as Lagrange–Euler equations

$$\frac{d}{dt}\left(\frac{\partial L}{\partial \dot{x}_c}\right) - \frac{\partial L}{\partial x_c} = 0, \qquad \frac{d}{dt}\left(\frac{\partial L}{\partial \dot{y}_c}\right) - \frac{\partial L}{\partial y_c} = 0, \tag{1.3}$$

where L is a Lagrangian of the form

$$L = \frac{\mu}{2}\big(\dot{x}_c^2 + \dot{y}_c^2\big) - U,$$

with $\mu = m + \rho\pi R^2$ being the effective mass and $U = U(x_c, y_c)$ the scalar potential

$$U = \frac{\rho q_1^2}{4\pi} \ln\left(1 - \frac{R^2}{(x_c + a)^2 + y_c^2}\right) + \frac{\rho q_2^2}{4\pi} \ln\left(1 - \frac{R^2}{(x_c - a)^2 + y_c^2}\right) + \\ + \frac{\rho q_1 q_2}{4\pi} \ln\left(1 + \frac{R^4 - 2R^2\big(x_c^2 + y_c^2 - a^2\big)}{\big((x_c + a)^2 + y_c^2\big)\big((x_c - a)^2 + y_c^2\big)}\right). \tag{1.4}$$

Hamiltonian form. Making the standard Legendre transformation, we represent the system (1.3) in the Hamiltonian form

$$\begin{aligned}
\dot{x}_c &= \frac{\partial H}{\partial p_x} = \frac{p_x}{\mu}, \qquad \dot{y}_c = \frac{\partial H}{\partial p_y} = \frac{p_y}{\mu}, \\
\dot{p}_x &= -\frac{\partial H}{\partial x_c} = -\frac{\rho q_1^2 R^2 (a + x_c)}{2\pi r_+^2 \big(r_+^2 - R^2\big)} + \frac{\rho q_2^2 R^2 (a - x_c)}{2\pi r_-^2 \big(r_-^2 - R^2\big)} - \\
&\quad - \frac{q_1 q_2 \rho R^2 x_c \Big(4a^2\big(4a^2 + R^2\big) - \big(8a^2 + R^2\big)\big(r_+^2 + r_-^2\big) + r_+^4 + r_-^4\Big)}{2\pi r_+^2 r_-^2 \Big(4R^2 a^2 + \big(r_-^2 - R^2\big)\big(r_+^2 - R^2\big)\Big)}, \\
\dot{p}_y &= -\frac{\partial H}{\partial y_c} = -\frac{\rho q_1^2 R^2 y_c}{2\pi r_+^2 \big(r_+^2 - R^2\big)} - \frac{\rho q_2^2 R^2 y_c}{2\pi r_-^2 \big(r_-^2 - R^2\big)} + \\
&\quad + \frac{q_1 q_2 \rho R^2 y_c \Big(\big(4a^2 + R^2\big)\big(r_+^2 + r_-^2\big) - r_+^4 - r_-^4\Big)}{2\pi r_+^2 r_-^2 \Big(4R^2 a^2 + \big(r_-^2 - R^2\big)\big(r_+^2 - R^2\big)\Big)}, \\
r_+^2 &= (a + x_c)^2 + y_c^2, \qquad r_-^2 = (a - x_c)^2 + y_c^2,
\end{aligned} \tag{1.5}$$

with the Hamiltonian

$$H = \frac{1}{2\mu}\left(p_x^2 + p_y^2\right) + U. \tag{1.6}$$

Thus, the problem reduces to investigating the motion of a material point (the geometric center of the foil) moving in a potential field U. Next, we turn to analysis of the surface of the potential and its singular points.

§ 2. Analysis of the system

In the general case, the motion of the system is defined by the potential (1.4), which has 5 parameters: the position of source a, the intensities of sources q_1 and q_2, the radius of the circular foil, R, and the fluid density ρ. Figure 2 presents an example of the surface of the potential U on different sides for $a = 2$ and for the following parameter values:

$$R = 1, \qquad q_1 = 5, \qquad q_2 = 1, \qquad \rho = 1. \tag{2.1}$$

Remark 2.1. For the system under consideration, by choosing units of measurement of mass, length and time, one can always achieve that $R = 1$, $|q_2| = 1$ and $\rho = 1$. As a result, there remain only two parameters a and q_1.

We note that the potential (1.4) has singularities and tends to $-\infty$ as it approaches the circles

$$(x_c \pm a)^2 + y_c^2 = R^2. \tag{2.2}$$

Inside the circles (2.2) the potential U is undefined. The contact of the center of the foil with any of the circles (2.2) corresponds to the contact of the boundary of the foil with one of the sources. The potential (1.4) is always negative for any values of x_c, y_c and the parameters. Also, the following asymptotics are valid for it:

$$\lim_{x_c^2+y_c^2\to\infty} U = -0.$$

Invariant manifolds and fixed points. The black dots in Fig. 2 indicate the critical points of the potential (1.4) which correspond to the fixed points of the system. In the general case, analysis of the fixed points reduces to finding the roots of a nonlinear system of equations that contains polynomials of orders 8 and 9 in the variables x_c and y_c. Therefore, the explicit solutions can be found only in particular cases (see Sections 2.1 and 2.2).

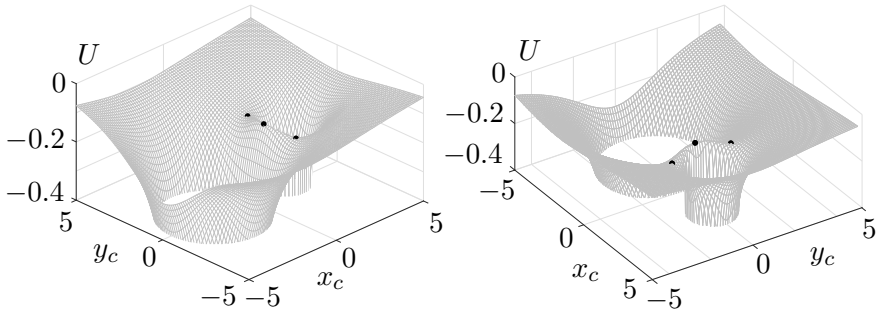

Fig. 2. The surface of the potential (1.4) for the parameters (2.1) (on different sides)

The system (1.5) admits the invariant manifold

$$p_y = 0, \qquad y_c = 0. \tag{2.3}$$

The motion on this manifold is given by the equations

$$\dot{x}_c = \frac{p_x}{\mu}, \qquad \dot{p}_x = -\frac{\rho q_1^2 R^2}{2\pi r_+\left(r_+^2 - R^2\right)} + \frac{\rho q_2^2 R^2}{2\pi r_-\left(r_-^2 - R^2\right)} - \frac{q_1 q_2 \rho R^2 x_c}{\pi r_+ r_-\left(R^2 + r_+ r_-\right)}, \tag{2.4}$$

where $r_+ = a + x_c$, $r_- = a - x_c$. The system (2.4) is defined on the following intervals:

$$x_c \in (-\infty, -a - R) \cup (-a + R, a - R) \cup (a + R, \infty) \quad \text{under the condition} \quad a > R,$$
$$x_c \in (-\infty, -a - R) \cup (a + R, \infty) \quad \text{under the condition} \quad a \leqslant R.$$

If x_c does not appear in the above-mentioned intervals, then this corresponds to contact of one or both sources with the boundary of the foil or with the interior of the foil. A phase portrait of the system for $m = 1$ and the parameters (2.1) is shown in Fig. 3.

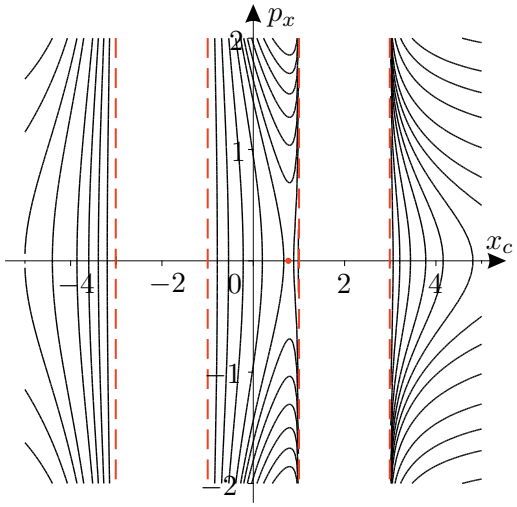

Fig. 3. Phase portrait of the system (2.4) for the parameters (2.1)

The red dotted lines in Fig. 3 indicate the boundaries of the phase portrait which correspond to contact of the foil with one of the sources. Also, the red dot in Fig. 3 indicates the fixed point of the system (2.4) with coordinates $(x_c^*, 0)$, where x_c^* is defined from the solution of the equation

$$-(q_1+q_2)^2 x_c^5 + 3a(q_1^2 - q_2^2)x_c^4 + 2(R^2(q_1+q_2)^2 - a^2(q_1-q_1)^2)x_c^3 - 2a(q_1^2-q_2^2)(2R^2+a^2)x_c^2 +$$
$$+ \left((3q_1^2 - 2q_1q_2 + 3q_2^2)a^4 + 2R^2a^2(q_1+q_2)^2 - R^4(q_1+q_2)^2\right)x_c - a^5(q_1^2-q_2^2) + aR^4(q_1^2-q_2^2) = 0.$$

It can be seen from the phase portrait that the system (2.4) has trajectories that are attracted to one of the singularities, and a fixed point.

The Hill regions. To investigate the system in general (not on the manifold), we construct characteristic examples of the Hill regions $U < E$ for different values of E. They show regions of bounded motions of the system. The Hill regions with parameters (2.1) and $a = 2$ are shown in Fig. 4.

It follows from Fig. 4 that for energies $E \leqslant 0$ all trajectories will be bounded. To realize the trajectories leading the cylinder to infinity, it is necessary to impart energy $E > 0$ to the system.

Basins of attraction. As noted above, the system under consideration has two types of trajectories: those going to infinity $\left(x_c^2 + y_c^2 \to \infty\right)$ and those attracted to one of the sources in finite time (the proofs of this statement are given in [12]). This behavior of the trajectories is typical of such systems (a circular foil and a source [13], a circular foil and a vortex source [12]).

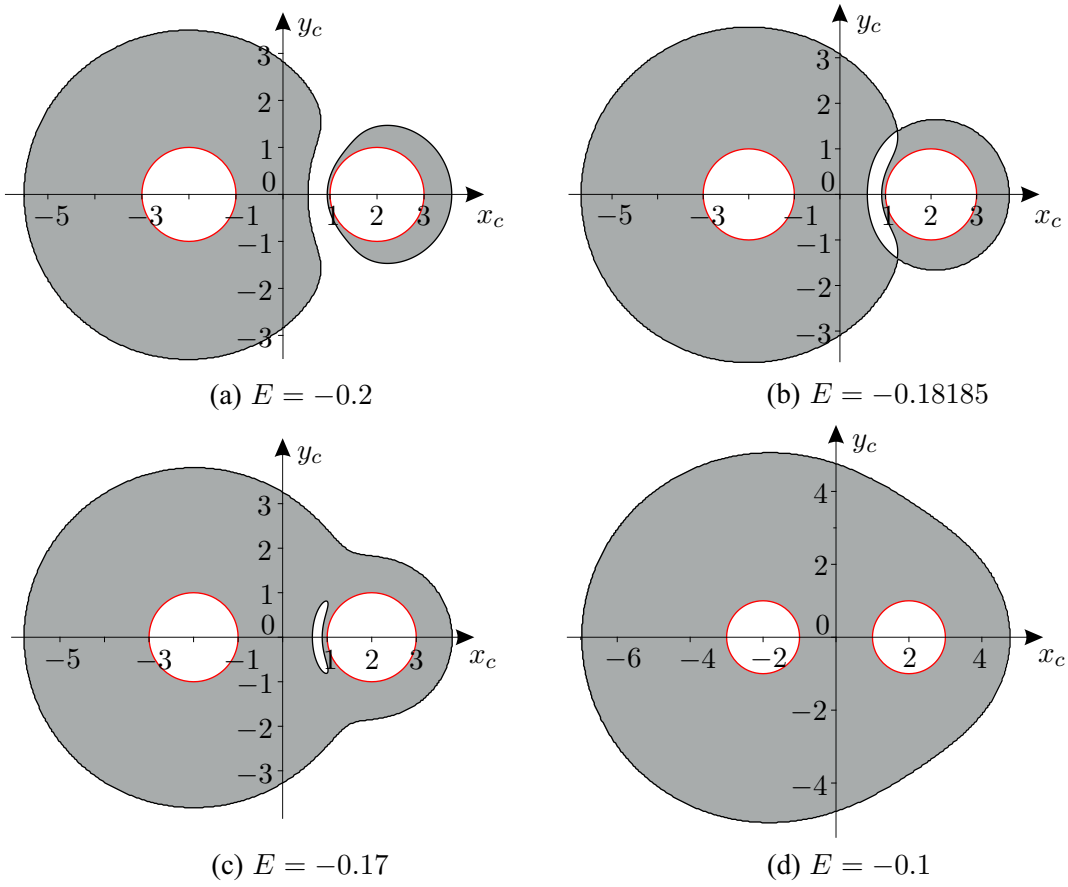

(a) $E = -0.2$ (b) $E = -0.18185$

(c) $E = -0.17$ (d) $E = -0.1$

Fig. 4. The Hill regions with parameters (2.1) and different E

Consider the system (1.5) in the case where all trajectories are bounded and are attracted to the sources, i. e., $U < E$. Figure 5 shows basins of attraction of the sources on the plane of initial conditions $\big(x_c(0), y_c(0)\big)$ for

$$p_x(0) = 0, \qquad p_y(0) = 0,$$

for the parameters (2.1), and $m = 1$. Dark gray denotes the region of attraction to the left source, and light gray represents the region of attraction to the right source. Red denotes the boundary of the region of possible motions (condition (2.2)) which corresponds to the fall of the foil onto one of the sources.

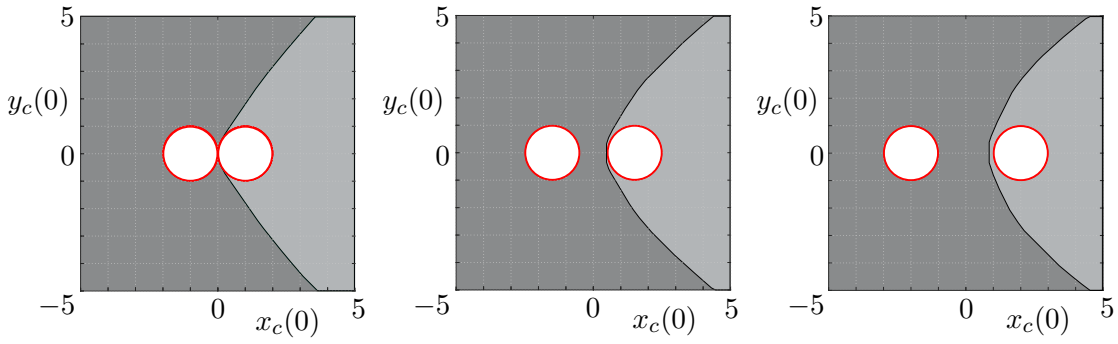

(a) $a = 1$ (b) $a = 1.5$ (c) $a = 2$

Fig. 5. Dependence of the attraction of the trajectory to the sources on the initial position

The black line in Fig. 5 indicates the curve separating the dark gray and the light gray region. Numerical experiments show that this line is smooth and presumably corresponds to

some invariant manifold on which the dynamics of the system is not asymptotic (that is, the trajectory is not attracted to the sources and does not go to infinity). Also, this curve has fixed points of the system (1.5). However, it is impossible to define the explicit form of the invariant manifold. Therefore, the question of the existence of this manifold and of investigating the dynamics of motion on it remains open.

Unbounded trajectories. The trajectories of the foil that lead it from the sources to infinity are possible if one imparts some positive energy to the foil to overcome the attraction of the sources. This can be achieved by specifying a nonzero initial velocity of the foil. Figure 6 shows, on the plane of initial conditions $\big(x_c(0), y_c(0)\big)$, regions where the circular foil goes to infinity (white region), and the regions of attraction to the sources (gray regions) for the parameters (2.1). The initial conditions for the momenta are given as

$$p_x(0) = -V\mu\cos\varphi, \qquad p_y(0) = -V\mu\sin\varphi, \tag{2.5}$$

where $\varphi = \arctan\big(y_c(0), x_c(0)\big)$, and V is the initial absolute value of the velocity. Conditions (2.5) have been chosen in such a way that the velocity vector of the foil at the initial time is always directed to point O (see Fig. 1).

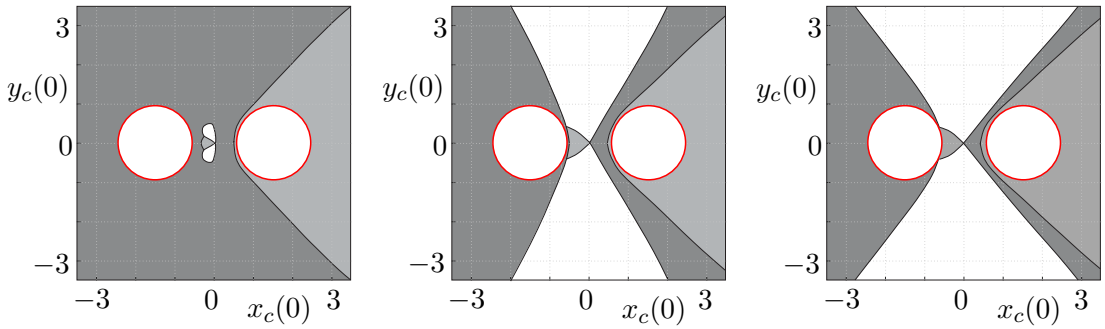

(a) $V = 1$ (b) $V = 2$ (c) $V = 3$

Fig. 6. Dependence of the attraction of the trajectory to the sources on the initial position for $a = 1.5$

Integrability. For arbitrary values of intensities q_1 and q_2, only numerical analysis of the system is possible. Since the trajectories of equations (1.5) are noncompact, it does not seem possible to use the method of a Poincaré map.

To investigate the system, the dependencies of the scattering angle θ and the deviation b_1 on the impact parameter b_0 were constructed (a detailed description of the procedure of constructing and the meaning of these quantities is given in **Appendix A**). Figures 7 and 8 show the dependencies $\theta(b_0)$ and $b_1(b_0)$, respectively, for $a = 2$, the parameters (2.1) and for different values of the energy integral E. The dotted lines in Figs. 7 and 8 denote the boundaries of regions in which the trajectories fall onto the singularities of the potential U.

It can be seen from Figs. 7 and 8 that the curves behave smoothly, which makes it impossible to determine whether the system is integrable or nonintegrable. Such diagrams were used in [16] and contained irregular fragments, providing a numerical proof of nonintegrability.

In addition to constructing the scattering angle for analysis of systems with noncompact trajectories, one can calculate the Kovalevskaya exponents [17] or the Melnikov integral [18] if one knows some particular solution of the unperturbed system. For the system under consideration, a calculation was made of the Kovalevskaya exponents (under the assumption that $x_c \gg a$ and $y_c \gg 0$) and of the Melnikov integral (q_1 and q_2 were taken to be perturbations). But the results did not make it possible to determine the dynamical behavior of the system either. Therefore, the question of integrability of the system remains open.

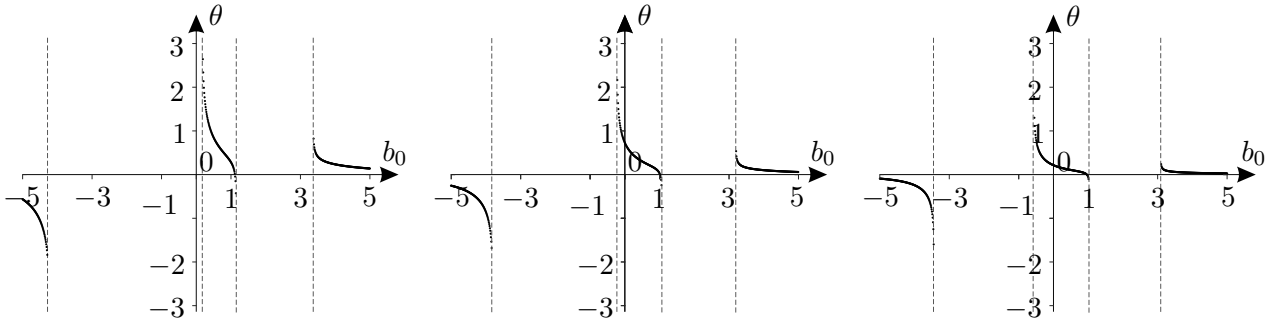

(a) $E = 1$ (b) $E = 2$ (c) $E = 5$

Fig. 7. Dependence of the scattering angle on the impact parameter b_0

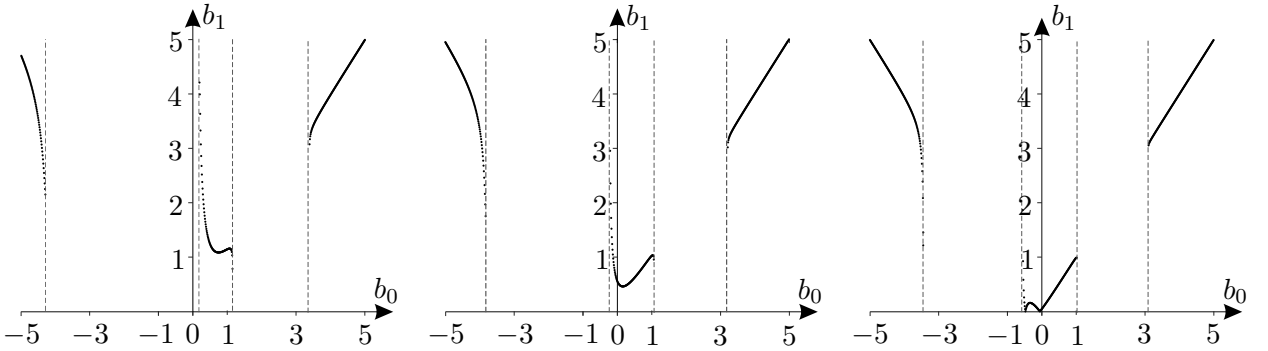

(a) $E = 1$ (b) $E = 2$ (c) $E = 5$

Fig. 8. Dependence of the deviation on the impact parameter b_0

Next, we turn our attention to particular cases: sources of the same intensity $q_1 = q_2$ and sources whose intensities have the same absolute value, but are opposite in sign: $q_1 = -q_2$.

2.1. The case $q_1 = q_2 = q$

For sources of the same intensity the numerical experiment has shown that the fixed points (the critical points of the potential (1.4)) can lie only on the straight lines $x_c = 0$ or $y_c = 0$ and can be found explicitly.

In the case $y_c = 0$ all fixed points lie on the invariant manifold (2.3) and the following holds:

$$\left.\frac{\partial U}{\partial y_c}\right|_{y_c=0} = \dot{p}_y\big|_{y_c=0} = 0.$$

Thus, to define the coordinate x_c of the fixed point, it is necessary to consider the equation

$$\left.\frac{\partial U}{\partial x_c}\right|_{y_c=0} = x_c\left(x_c^4 - 2R^2x_c^2 + R^4 - 2R^2a^2 - a^4\right) = 0.$$

This equation has several roots:

$$x_c = 0, \qquad x_c = \pm\sqrt{R^2 \pm \sqrt{a^4 + 2R^2a^2}},$$

but only one root, $x_c = 0$, has a physical meaning. Thus, one of the critical points of the potential (1.4) is given as

$$x_c = 0, \qquad y_c = 0. \tag{2.6}$$

This point exists only for $a > R$ and is always unstable but, depending on the system's parameters, can change type (saddle or saddle-center). Point (2.6) corresponds to finding the foil from the center between the sources (see Fig. 9, *a*).

In the case $x_c = 0$ the following holds:

$$\left.\frac{\partial U}{\partial x_c}\right|_{x_c=0} = \dot{p}_x\big|_{x_c=0} = 0.$$

The equation for the coordinate y_c of the fixed point has the form

$$\left.\frac{\partial U}{\partial y_c}\right|_{x_c=0} = y_c\left(y_c^4 - 2R^2y_c^2 + R^4 + 2R^2a^2 - a^4\right) = 0.$$

The solutions that are nonzero and satisfy the conditions $(x_c \pm a)^2 + y_c^2 > R^2$ have the following form:

- $y_c = \pm\sqrt{R^2 + \sqrt{a^4 - 2R^2a^2}}$, these solutions exist for $a > \sqrt{2}R$. Regardless of the parameter values, the point is unstable (a saddle). The position of the foil corresponding to this solution is shown in Fig. 9, *b*.
- $y_c = \pm\sqrt{R^2 - \sqrt{a^4 - 2R^2a^2}}$, these solutions exist for $a \in (\sqrt{2}R, \sqrt{1+\sqrt{2}}R)$. This fixed point is also unstable (a saddle-center). The position of the foil corresponding to this solution is shown in Fig. 9, *c*.

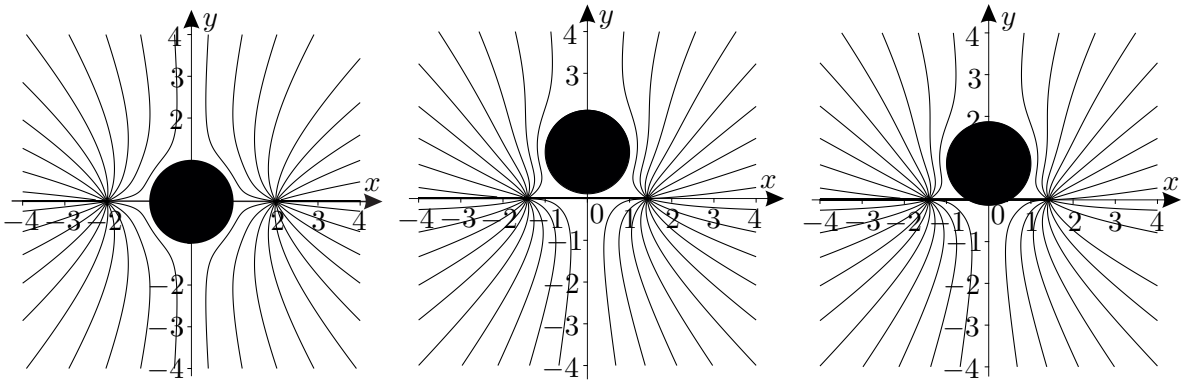

Fig. 9. Equilibrium points of the foil of radius $R = 1$ which correspond to a fixed point: (a) $(0, 0)$ for $a = 2$, (b) $(0, \sqrt{R^2 + \sqrt{a^4 - 2R^2a^2}})$, and (c) $(0, \sqrt{R^2 - \sqrt{a^4 - 2R^2a^2}})$ for $a = \sqrt{2} + 0.01$ together with streamlines

Thus, for the parameter $a > R$, the system either has 1, 3 or 5 fixed points or in the case the parameter $a \leqslant R$ it has no fixed points at all (a schematic diagram is presented in Fig. 10). The continuous lines in Fig. 10 represent points of saddle type, and the dotted lines indicate saddle-center points. Changes that occur in the surface of the potential U as a varies with the parameters

$$m = 1, \qquad \rho = 1, \qquad q_1 = 1, \qquad q_2 = 1$$

are shown in Fig. 11.

Although the above-mentioned solutions were found only in particular cases for $x_c = 0$ or $y_c = 0$, numerical experiments show that the potential (1.4) has no other critical points for $q_1 = q_2 = q$. However, a rigorous proof of this statement remains an open question.

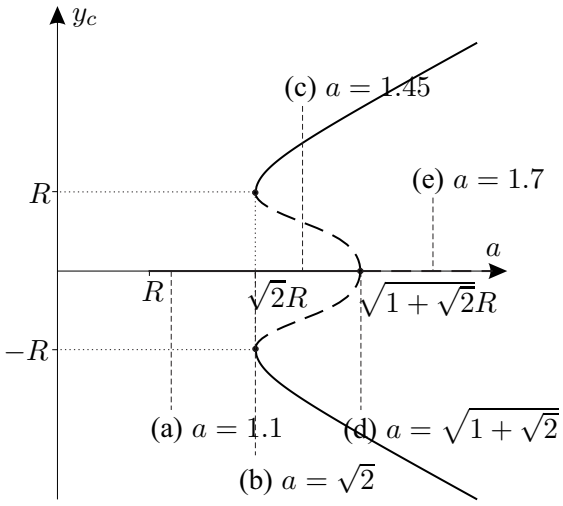

Fig. 10. Bifurcation diagram

2.2. The case $q_1 = -q_2 = q$

If the intensities of the sources have the same absolute value, but are opposite in sign, analysis of equations (1.6) for the fixed points reduces to analysis of the following system of equations:

$$\begin{cases} x_c\big(R^2 + a^2 - x_c^2 - y_c^2\big) = 0, \\ y_c\big(R^2 - a^2 - x_c^2 - y_c^2\big) = 0. \end{cases} \tag{2.7}$$

The system (2.7) has only one physically meaningful solution $x_c = 0$, $y_c = 0$ (the position of the foil in Fig. 12). This fixed point exists only for $a > R$ and is always an unstable point of saddle type.

In the case $q_1 = -q_2 = q$ we consider here, there exists a passage to the limit $a \to 0$ that leads to analysis of the problem of the motion of a balanced circular foil in the field of a fixed point dipole. We consider this system in the next section.

§ 3. A circular foil with a dipole

Let us relate the intensities of sources q_1 and q_2 to their positions as follows:

$$q_1 = \frac{M}{2a}, \qquad q_2 = -\frac{M}{2a},$$

where M is the quantity characterizing the intensity of the dipole (strength of the dipole). Substituting these relations into equations (1.6) and assuming that $a \to 0$, we obtain equations of motion for the circular foil in the field of a fixed dipole

$$\begin{aligned} \dot{x}_c &= \frac{\partial H}{\partial p_x} = \frac{p_x}{\mu}, & \dot{y}_c &= \frac{\partial H}{\partial p_y} = \frac{p_x}{\mu}, \\ \dot{p}_x &= -\frac{\partial H}{\partial x_c} = \frac{\rho M^2 R^2 x_c}{\pi\big(R^2 - x_c^2 - y_c^2\big)^3}, & \dot{p}_y &= -\frac{\partial H}{\partial y_c} = \frac{\rho M^2 R^2 y_c}{\pi\big(R^2 - x_c^2 - y_c^2\big)^3}, \end{aligned} \tag{3.1}$$

with the Hamiltonian

$$H = \frac{1}{2\mu}\big(p_x^2 + p_y^2\big) - \frac{\rho M^2 R^2}{4\pi\big(R^2 - x_c^2 - y_c^2\big)^2}.$$

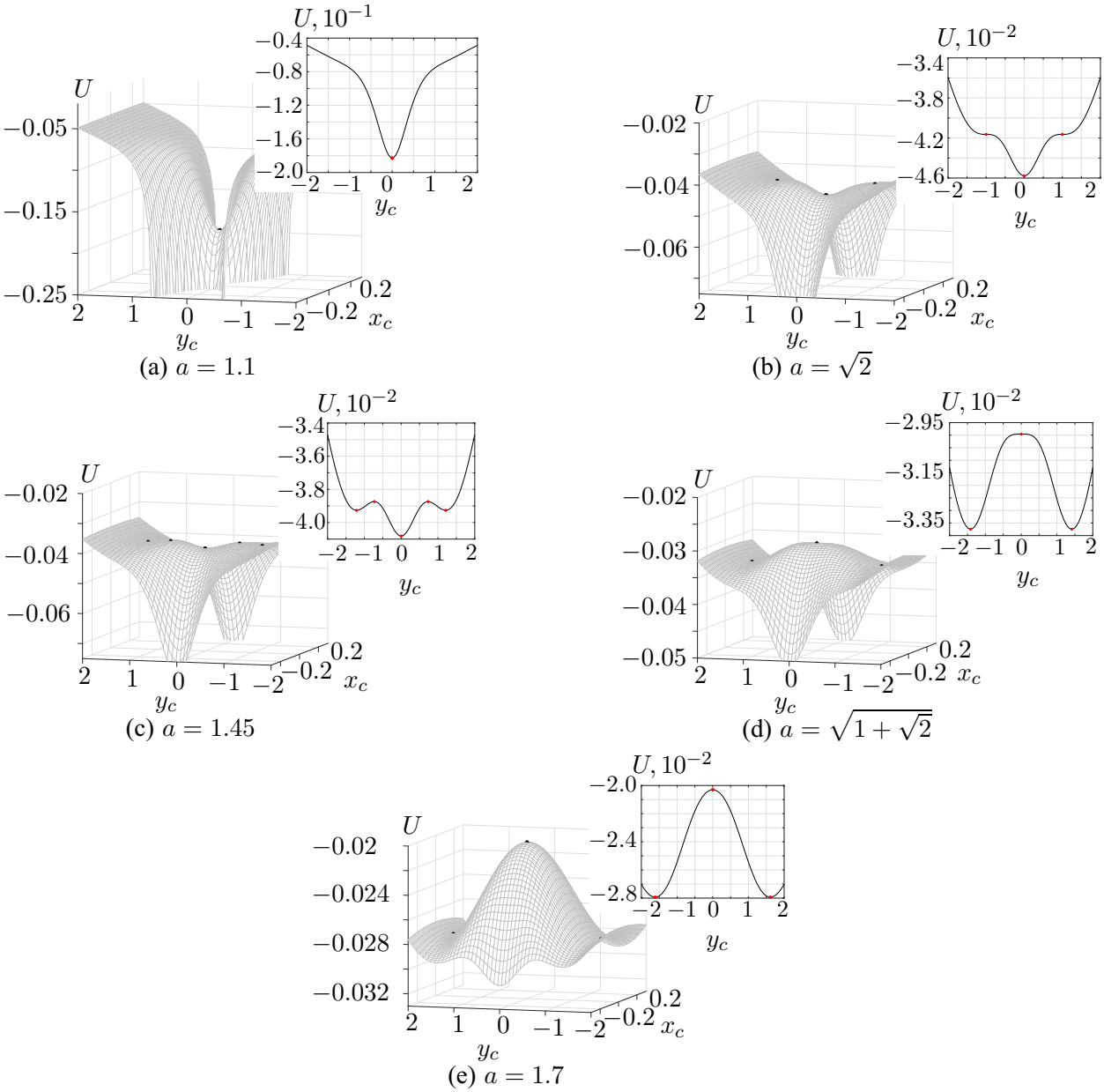

Fig. 11. Surfaces of the potential U for $R = 1$ and different values of the parameter a and sections formed by the intersection of this surface with the plane $x_c = 0$

Remark 3.1. Equations (3.1) can be obtained from the Newton–Euler equations with the force calculated by the Sedov formula (1.1) using the complex potential

$$w = -\frac{uR^2}{z - z_c} - \frac{M}{2\pi z} - \frac{M(z - z_c)}{2\pi \overline{z_c}(z - z_d^*)}, \qquad z_d^* = z_c - \frac{R^2}{\overline{z_c}}.$$

Here the first term describes the motion of a cylinder with velocity u, the second describes the presence of a dipole at the origin in the fluid, and the third term follows from the Milne–Thomson circle theorem.

The system of equations (3.1) admits an integral of the angular momentum of the form

$$K = p_y x_c - p_x y_c. \tag{3.2}$$

Next, we perform a reduction to the fixed level set of this integral.

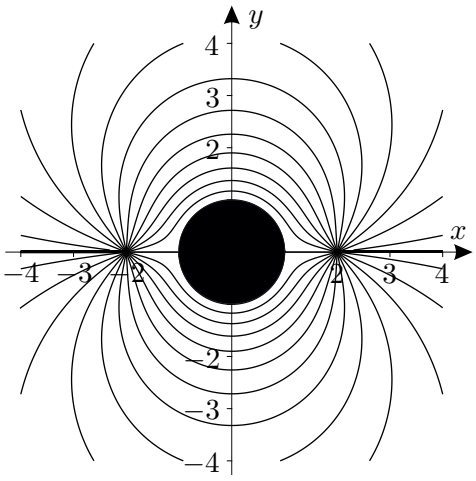

Fig. 12. Equilibrium points of a foil of radius $R = 1$ which correspond to the fixed point $(0, 0)$ with $a = 2$ together with streamlines

Reduction. For reduction we transform to polar coordinates in a standard way and introduce new momenta

$$x_c = r\cos\varphi, \quad y_c = r\sin\varphi, \quad p_r = p_x\cos\varphi + p_y\sin\varphi, \quad p_\varphi = K = r(-p_x\sin\varphi + p_y\cos\varphi).$$

Then, in the new variables, equations (3.1) become

$$\dot r = \frac{\partial H}{\partial p_r} = \frac{p_r}{\mu}, \qquad \dot\varphi = \frac{\partial H}{\partial p_\varphi} = \frac{p_\varphi}{\mu r^2},$$
$$\dot p_r = -\frac{\partial H}{\partial r} = \frac{p_\varphi^2}{\mu r^3} + \frac{R^2M^2\rho r}{\pi\left(R^2 - r^2\right)^3}, \quad \dot p_\varphi = -\frac{\partial H}{\partial\varphi} = 0,$$

with the Hamiltonian

$$H = \frac{1}{2\mu r^2}\left(r^2p_r^2 + p_\varphi^2\right) - \frac{\rho R^2M^2}{4\pi\left(R^2 - r^2\right)^2}.$$

It can be seen that the right-hand side of the equation for the variable p_φ corresponding to the integral (3.2) vanishes and the variable φ conjugate to p_φ is cyclic.

Let us fix the value $p_\varphi = K = k$ and proceed to analyze the system on the fixed level set of the integral

$$\dot r = \frac{p_r}{\mu}, \qquad \dot p_r = \frac{k^2}{\mu r^3} + \frac{R^2M^2\rho r}{\pi\left(R^2 - r^2\right)^3}. \tag{3.3}$$

Next, we address the question of the existence of particular solutions of this system.

Fixed points. It follows from equations (3.3) that the fixed points can lie only on the straight line $p_r = 0$. To define the coordinate r of the fixed points, it is necessary to solve the following equation:

$$l^3 - \frac{R^2\left(\pi\rho^2M^2R^2 + m\rho M^2 + 3\pi k^2\right)}{\pi k^2}l^2 + 3R^4l - R^6 = 0, \tag{3.4}$$

where $l = r^2$. By analyzing this equation using Cardano's formula, it can be shown that equation (3.4) with $k \neq 0$ always has one real root and two complex conjugate roots. In the case $k = 0$

the right-hand side of the equation, $\dot{p}_r$, vanishes only if $r = 0$, which corresponds to coincidence of the geometric center of the foil and the dipole.

For the problem at hand, with k arbitrary, it is only the roots satisfying the inequality $r > R > 0$ that have a physical meaning. Therefore, when $k = 0$, the system has no fixed points. To analyze the solutions for $k \neq 0$, we make the change of variables $s = l - R^2$ and pass to the equation

$$s^3 - \frac{\rho\mu M^2 R^2}{\pi k^2} s^2 - \frac{2\rho\mu M^2 R^4}{\pi k^2} s - \frac{\rho\mu M^2 R^6}{\pi k^2} = 0. \tag{3.5}$$

According to the Vièta's formulas, the free term in equation (3.5) with $k \neq 0$ and $M \neq 0$ is always negative, and hence the product of the roots is always positive. As noted above, two roots of the equation are complex conjugate, one is real, and hence the real root is always positive.

Phase portraits. According to the analysis of the fixed points, the system (3.3) has two qualitatively different phase portraits. Figure 13 shows phase portraits for the following parameter values:

$$\begin{gathered} M = 1, \qquad R = 1, \qquad m = 1, \qquad \rho = 1, \\ \text{(a)}\ \ k = 0, \qquad \text{(b)}\ \ k = 1. \end{gathered} \tag{3.6}$$

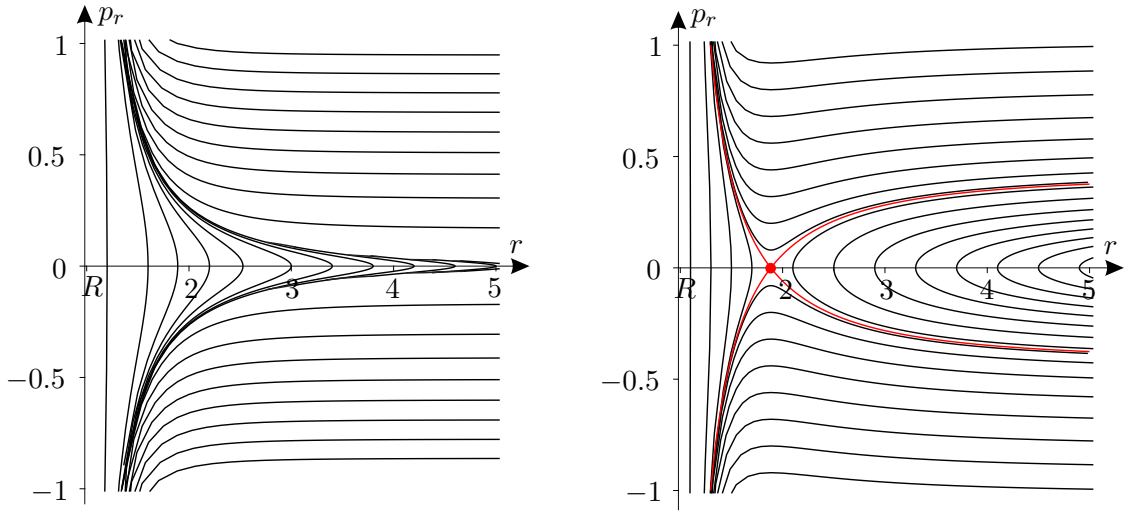

Fig. 13. Phase portraits of the system (3.3) with the parameters (3.6)

The red dot in the phase portraits indicates an unstable fixed point corresponding to motion about the dipole. It can be seen from the phase portraits that, in addition to the periodic trajectory, the system has the following trajectories:

- those coming from infinity and going to infinity;
- those coming from infinity and falling onto the dipole;
- those emanating from the singularity and falling onto it.

The difference of the system with a dipole from the system with a fixed source [13] is that an unstable fixed point arises at any nonzero value of the integral of angular momentum k. Otherwise the dynamics of the system is similar to that found in [13].

Conclusion

This paper is concerned with the motion of a balanced circular foil in the field of two fixed point sources. It is shown that the motion of the foil is described by a Hamiltonian system with two degrees of freedom and reduces to analysis of the motion of a material point in a potential field. In particular cases, we find critical points of the potential or, which is the same, fixed points of the system, which are always unstable. The question of integrability of such a system remains open at present.

An analysis is made of the limiting case for two sources whose intensities are opposite in sign, but have the same absolute value and which are infinitely close to each other. In other words, the case of motion of a circular foil in the field of a fixed dipole is considered. It is shown that in this case the system has an additional integral of angular momentum and hence the problem is integrable. An analysis of the fixed points of the system is carried out and typical phase portraits are presented.

The authors extend their gratitude to A. A. Kilin and E. V. Vetchanin for discussions of the results and a careful reading of the paper.

Appendix A

Construction of a scattering angle allows a qualitative estimate of the sensitivity of the trajectory to a small change in the initial condition (the impact parameter b_0). Abrupt (nonsmooth) changes in the scattering angle on a small interval of the impact parameter suggest that the system exhibits chaotic behavior [16].

In this work, the scattering angle θ and the deviation b_1 after scattering were constructed in accordance with the scheme presented in Fig. 14, i. e., the trajectories were started from the straight line parallel to the axis Ox_c. It should be noted that a comprehensive study requires addressing the question of the dependence of the behavior of the trajectories on the direction in which they are started (for example, from the straight line parallel to the axis Oy_c). But numerical experiments show that, for the system under consideration, changes in the initial position/direction do not lead to qualitatively different results.

We describe the algorithm for constructing the dependencies $\theta(b_0)$ and $b_1(b_0)$. In the region remote from singularities where the value of the potential is close to zero and changes only slightly, the following initial conditions are chosen:

$$\big(x_c(0), y_c(0)\big) = \big(b_0^{(k)}, y_0\big), \qquad k = 1, \dots, n,$$

where $b_0^{(1)}, \dots, b_0^{(n)}$ are the impact parameters and y_0 is such that $U\big(x_c = b_0^{(k)}, y_c = y_0\big) \approx 0$ (see Fig. 14). In the calculations presented in Section 2, $y_0 = -30$, and the initial velocities are chosen to be $(\dot{x}_c(0), \dot{y}_c(0)) = (0, v)$, where v is calculated from the total energy

$$E = \frac{\mu v^2}{2} + U\Big|_{x_c = b_0^{(k)},\ y_c = y_0}, \qquad E = \text{const}.$$

The chosen initial conditions are used for numerical integration of the system

$$\mu\ddot{x}_c = -\frac{\partial U}{\partial x_c}, \qquad \mu\ddot{y}_c = -\frac{\partial U}{\partial y_c}.$$

The scattering angle θ is calculated by choosing time T such that at $t > T$ the motion of the system is close to rectilinear, i. e., $U\big(x_c(T), y_c(T)\big) \approx 0$ and $\operatorname{grad} U \approx 0$. Since the system under consideration has trajectories falling onto singularities (2.2), in further calculations we will be interested in trajectories that have interacted with the singularities, but have not been attracted

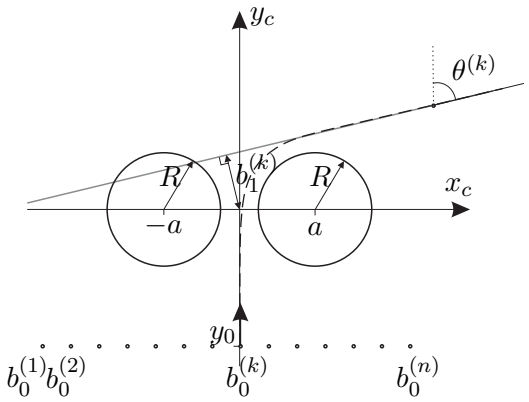

Fig. 14. Schematic representation of scattering

to them. The scattering angle θ_k for each impact parameter $b_0^{(k)}$ is defined by the formulae (see Fig. 14)

$$\theta_k = -\arctan\frac{\dot{x}_c(T)}{\dot{y}_c(T)},$$

and the deviation of the trajectory $b_1^{(k)}$ (see Fig. 14) for each $b_0^{(k)}$ is calculated as the distance from point (0, 0) to the straight line which the trajectory has reached at $t > T$.

Funding. The work of E. M. Artemova was carried at the Ural Mathematical Center (Agreement No. 075–02–2025–1609). The work of D. A. Lagunov was carried out within the framework of the state assignment of the Ministry of Science and Higher Education of the Russian Federation (FEWS–2024–0007).

REFERENCES

1. Eldredge J. D. Numerical simulation of the fluid dynamics of 2D rigid body motion with the vortex particle method, *Journal of Computational Physics*, 2007, vol. 221, issue 2, pp. 626–648. https://doi.org/10.1016/j.jcp.2006.06.038
2. Herreros M. I., Ligüérzana S. Rigid body motion in viscous flows using the finite element method, *Physics of Fluids*, 2020, vol. 32, issue 12, 123311. https://doi.org/10.1063/5.0029242
3. Wang Z. J., Birch J. M., Dickinson M. H. Unsteady forces and flows in low Reynolds number hovering flight: two-dimensional computations vs robotic wing experiments, *Journal of Experimental Biology*, 2004, vol. 207, issue 3, pp. 449–460. https://doi.org/10.1242/jeb.00739
4. Kanso E., Marsden J. E., Rowley C. W., Melli-Huber J. B. Locomotion of articulated bodies in a perfect fluid, *Journal of Nonlinear Science*, 2005, vol. 15, issue 4, pp. 255–289. https://doi.org/10.1007/s00332-004-0650-9
5. Klekovkin A. V., Karavaev Y. L., Kilin A. A., Nazarov A. V. The influence of tail fins on the speed of an aquatic robot driven by internal moving masses, *Computer Research and Modeling*, 2024, vol. 16, no. 4, pp. 869–882 (in Russian). https://doi.org/10.20537/2076-7633-2024-16-4-869-882
6. Klekovkin A. V., Karavaev Y. L., Mamaev I. S. The control of an aquatic robot by a periodic rotation of the internal flywheel, *Russian Journal of Nonlinear Dynamics*, 2023, vol. 19, no. 2, pp. 265–279. https://doi.org/10.20537/nd230301
7. Karavaev Y. L., Klekovkin A. V., Mamaev I. S., Tenenev V. A., Vetchanin E. V. A simple physical model for control of an propellerless aquatic robot, *Journal of Mechanisms and Robotics*, 2022, vol. 14, no. 1, 011007. https://doi.org/10.1115/1.4051240
8. Ramodanov S. M., Sokolov S. V. Dynamics of a circular cylinder and two point vortices in a perfect fluid, *Regular and Chaotic Dynamics*, 2021, vol. 26, no. 6, pp. 675–691. https://doi.org/10.1134/S156035472106006X

9. Shashikanth B. N., Marsden J. E., Burdick J. W., Kelly S. D. The Hamiltonian structure of a two-dimensional rigid circular cylinder interacting dynamically with N point vortices, *Physics of Fluids*, 2002, vol. 14, issue 3, pp. 1214–1227. https://doi.org/10.1063/1.1445183
10. Mamaev I. S., Bizyaev I. A. Dynamics of an unbalanced circular foil and point vortices in an ideal fluid, *Physics of Fluids*, 2021, vol. 33, issue 8, 087119. https://doi.org/10.1063/5.0058536
11. Kilin A. A., Gavrilova A. M., Artemova E. M. Dynamics of an elliptic foil with an attached vortex in an ideal fluid: the integrable case, *Regular and Chaotic Dynamics*, 2025, vol. 30, issue 6, pp. 931–951. https://doi.org/10.1134/S1560354724590015
12. Artemova E. M., Vetchanin E. V. The motion of a circular foil in the field of a fixed point singularity: integrability and asymptotic behavior, *Physics of Fluids*, 2024, vol. 36, issue 2, 027139. https://doi.org/10.1063/5.0185865
13. Artemova E. M., Vetchanin E. V. The motion of an unbalanced circular disk in the field of a point source, *Regular and Chaotic Dynamics*, 2022, vol. 27, no. 1, pp. 24–42. https://doi.org/10.1134/S1560354722010051
14. Artemova E. M., Lagunov D. A., Vetchanin E. V. The motion of an elliptic foil in the field of a fixed vortex source, *Russian Journal of Nonlinear Dynamics*, 2025, vol. 21, no. 2, pp. 135–155. https://doi.org/10.20537/nd241203
15. Sedov L. I. *Two-dimensional problems in hydrodynamics and aerodynamics*, New York–London–Sydney: Interscience Publishers, 1965. https://zbmath.org/0131.40901
16. Ott E., Tél T. Chaotic scattering: an introduction, *Chaos*, 1993, vol. 3, issue 4, pp. 417–426. https://doi.org/10.1063/1.165949
17. Borisov A. V., Kilin A. A., Mamaev I. S. Hamiltonicity and integrability of the Suslov problem, *Regular and Chaotic Dynamics*, 2011, vol. 16, nos. 1–2, pp. 104–116. https://doi.org/10.1134/S1560354711010035
18. Mel'nikov V. K. On the stability of the center for time-periodic perturbations, *Transactions of the Moscow Mathematical Society*, 1963, vol. 12, pp. 1–56. https://zbmath.org/0135.31001

Received 01.09.2025
Accepted 25.10.2025

Elizaveta Markovna Artemova, Ural Mathematical Center, Udmurt State University, ul. Universitetskaya, 1, Izhevsk, 426034, Russia.
ORCID: https://orcid.org/0000-0001-7637-2757
E-mail: artemova@rcd.ru

Danil Arkad'evich Lagunov, Ural Mathematical Center, Udmurt State University, ul. Universitetskaya, 1, Izhevsk, 426034, Russia.
ORCID: https://orcid.org/0009-0004-4662-9231
E-mail: 1deqos23@gmail.com

Citation: E. M. Artemova, D. A. Lagunov. The motion of a balanced circular foil in the field of fixed point sources, *Vestnik Udmurtskogo Universiteta. Matematika. Mekhanika. Komp'yuternye Nauki*, 2025, vol. 35, issue 4, pp. 601–618.

МЕХАНИКА 2025. Т. 35. Вып. 4. С. 601–618.

Е. М. Артемова, Д. А. Лагунов

Движение уравновешенного кругового профиля в поле неподвижных точечных источников

Ключевые слова: идеальная жидкость, круговой профиль, точечный источник, гамильтонова форма.

УДК 532.5.031

DOI: 10.35634/vm250406

В данной работе рассматривается движение кругового профиля в идеальной несжимаемой жидкости, в которой находится два неподвижных точечных источника. Показано, что исследование такой системы сводится к исследованию движения материальной точки (геометрического центра профиля) в потенциальном поле. Указаны неподвижные точки системы, соответствующие стационарным конфигурациям профиля в абсолютном пространстве. Рассмотрен предельный случай, когда источники имеют противоположные по знаку, но одинаковые по модулю, интенсивности и стянуты в одну точку, то есть рассмотрено движение профиля в поле неподвижного диполя. Показано, что в этом случае система интегрируема, выполнен ее полный анализ.

Финансирование. Работа Артемовой Е. М. выполнена в Уральском математическом центре (соглашение № 075–02–2025–1609). Работа Лагунова Д. А. выполнена в рамках государственного задания Минобрнауки России (FEWS–2024–0007).

СПИСОК ЛИТЕРАТУРЫ

1. Eldredge J. D. Numerical simulation of the fluid dynamics of 2D rigid body motion with the vortex particle method // Journal of Computational Physics. 2007. Vol. 221. Issue 2. P. 626–648. https://doi.org/10.1016/j.jcp.2006.06.038
2. Herreros M. I., Ligüérzana S. Rigid body motion in viscous flows using the finite element method // Physics of Fluids. 2020. Vol. 32. Issue 12. 123311. https://doi.org/10.1063/5.0029242
3. Wang Z. J., Birch J. M., Dickinson M. H. Unsteady forces and flows in low Reynolds number hovering flight: two-dimensional computations vs robotic wing experiments // Journal of Experimental Biology. 2004. Vol. 207. Issue 3. P. 449–460. https://doi.org/10.1242/jeb.00739
4. Kanso E., Marsden J. E., Rowley C. W., Melli-Huber J. B. Locomotion of articulated bodies in a perfect fluid // Journal of Nonlinear Science. 2005. Vol. 15. Issue 4. P. 255–289. https://doi.org/10.1007/s00332-004-0650-9
5. Клековкин А. В., Караваев Ю. Л., Килин А. А., Назаров А. В. Влияние хвостовых плавников на скорость водного робота, приводимого в движение внутренними подвижными массами // Компьютерные исследования и моделирование. 2024. Т. 16. № 4. С. 869–882. https://doi.org/10.20537/2076-7633-2024-16-4-869-882
6. Klekovkin A. V., Karavaev Y. L., Mamaev I. S. The control of an aquatic robot by a periodic rotation of the internal flywheel // Russian Journal of Nonlinear Dynamics. 2023. Vol. 19. No. 2. P. 265–279. https://doi.org/10.20537/nd230301
7. Karavaev Y. L., Klekovkin A. V., Mamaev I. S., Tenenev V. A., Vetchanin E. V. A simple physical model for control of an propellerless aquatic robot // Journal of Mechanisms and Robotics. 2022. Vol. 14. No. 1. 011007. https://doi.org/10.1115/1.4051240
8. Ramodanov S. M., Sokolov S. V. Dynamics of a circular cylinder and two point vortices in a perfect fluid // Regular and Chaotic Dynamics. 2021. Vol. 26. No. 6. P. 675–691. https://doi.org/10.1134/S156035472106006X
9. Shashikanth B. N., Marsden J. E., Burdick J. W., Kelly S. D. The Hamiltonian structure of a two-dimensional rigid circular cylinder interacting dynamically with N point vortices // Physics of Fluids. 2002. Vol. 14. Issue 3. P. 1214–1227. https://doi.org/10.1063/1.1445183
10. Mamaev I. S., Bizyaev I. A. Dynamics of an unbalanced circular foil and point vortices in an ideal fluid // Physics of Fluids. 2021. Vol. 33. Issue 8. 087119. https://doi.org/10.1063/5.0058536

11. Kilin A. A., Gavrilova A. M., Artemova E. M. Dynamics of an elliptic foil with an attached vortex in an ideal fluid: The integrable case // Regular and Chaotic Dynamics. 2025. Vol. 30. Issue 6. P. 931–951. https://doi.org/10.1134/S1560354724590015
12. Artemova E. M., Vetchanin E. V. The motion of a circular foil in the field of a fixed point singularity: integrability and asymptotic behavior // Physics of Fluids. 2024. Vol. 36. Issue 2. 027139. https://doi.org/10.1063/5.0185865
13. Artemova E. M., Vetchanin E. V. The motion of an unbalanced circular disk in the field of a point source // Regular and Chaotic Dynamics. 2022. Vol. 27. No. 1. P. 24–42. https://doi.org/10.1134/S1560354722010051
14. Artemova E. M., Lagunov D. A., Vetchanin E. V. The motion of an elliptic foil in the field of a fixed vortex source // Russian Journal of Nonlinear Dynamics. 2025. Vol. 21. No. 2. P. 135–155. https://doi.org/10.20537/nd241203
15. Седов Л. И. Плоские задачи гидродинамики и аэродинамики. М.: Гостехиздат, 1950.
16. Ott E., Tél T. Chaotic scattering: An introduction // Chaos. 1993. Vol. 3. Issue 4. P. 417–426. https://doi.org/10.1063/1.165949
17. Borisov A. V., Kilin A. A., Mamaev I. S. Hamiltonicity and integrability of the Suslov problem // Regular and Chaotic Dynamics. 2011. Vol. 16. Nos. 1–2. P. 104–116. https://doi.org/10.1134/S1560354711010035
18. Мельников В. К. Об устойчивости центра при периодических по времени возмущениях // Труды Московского математического общества. 1963. Т. 12. С. 3–52. https://www.mathnet.ru/rus/mmo137

Поступила в редакцию 01.09.2025
Принята к публикации 25.10.2025

Артемова Елизавета Марковна, Уральский математический центр, Удмуртский государственный университет, 426034, Россия, г. Ижевск, ул. Университетская, 1.
ORCID: https://orcid.org/0000-0001-7637-2757
E-mail: artemova@rcd.ru

Лагунов Данил Аркадьевич, Уральский математический центр, Удмуртский государственный университет, 426034, Россия, г. Ижевск, ул. Университетская, 1.
ORCID: https://orcid.org/0009-0004-4662-9231
E-mail: 1deqos23@gmail.com

Цитирование: Е. М. Артемова, Д. А. Лагунов. Движение уравновешенного кругового профиля в поле неподвижных точечных источников // Вестник Удмуртского университета. Математика. Механика. Компьютерные науки. 2025. Т. 35. Вып. 4. С. 601–618.